

# Numerical Optimization by Finite Element Method of Stainless Steel/Glass-Epoxy Composite Bolted Joint under Tension and Compression

Christian Schmitt, Arnaud Kremer, Pawel Lipinski, Julien Capelle

National Engineering School of Metz, University of Lorraine, Metz, France  
Email: christian.schmitt@univ-lorraine.fr

**How to cite this paper:** Schmitt, C., Kremer, A., Lipinski, P. and Capelle, J. (2024) Numerical Optimization by Finite Element Method of Stainless Steel/Glass-Epoxy Composite Bolted Joint under Tension and Compression. *Engineering*, 16, 102-122.  
<https://doi.org/10.4236/eng.2024.164009>

**Received:** December 5, 2023  
**Accepted:** April 27, 2024  
**Published:** April 30, 2024

Copyright © 2024 by author(s) and Scientific Research Publishing Inc.  
This work is licensed under the Creative Commons Attribution International License (CC BY 4.0).  
<http://creativecommons.org/licenses/by/4.0/>



Open Access

---

## Abstract

The aim of this study was to optimize the geometry and the design of metallic/composite single bolted joints subjected to tension-compression loading. For this purpose, it was necessary to evaluate the stress state in each component of the bolted joint. The multi-material assembly was based on the principle of double lap bolted joint. It was composed of a symmetrical balanced woven glass-epoxy composite material plate fastened to two stainless sheets using a stainless pre-stressed bolt. In order to optimize the design and the geometry of the assembly, ten configurations were proposed and studied: a classical simple bolted joint, two joints with an insert (a BigHead<sup>®</sup> insert and a stair one) embedded in the composite, two “waved” solutions, three symmetrical configurations composed of a succession of metallic and composites layers, without a sleeve, with one and with two sleeves, and two non-symmetrical constituted of metallic and composites layers associated with a stair-insert (one with a sleeve and one without). A tridimensional Finite Element Method (FEM) was used to model each configuration mentioned above. The FE models took into account the different materials, the effects of contact between the different sheets of the assembly and the pre-stress in the bolt. The stress state was analyzed in the composite part. The concept of stress concentration factor was used in order to evaluate the stress increase in the highly stressed regions and to compare the ten configurations studied. For this purpose, three stress concentration factors were defined: one for a monotonic loading in tension, another for a monotonic loading in compression, and the third for a tension-compression cyclic loading. The results of the FEM computations showed that the use of alternative metallic and composite layers associated with two sleeves gived low values of stress concentration factors, smaller than

---

1.4. In this case, there was no contact between the bolt and the composite part and the most stressed region was not the vicinity of the hole but the end of the longest layers of the metallic inserts.

### **Keywords**

Bolted Joint, Glass-Epoxy Composite, Clearance, Hybrid Steel-Composite

---

### **Highlight**

- Ten configurations of stainless steel/woven glass-epoxy bolted joints were modelled using finite element method.
- Stress concentration factors were evaluated in the composite material under tension and compression loads.
- The best solution is a hybrid composite bolted joint with alternative stainless steel and glass-epoxy plies and with two sleeves.

## **1. Introduction**

For the past decades, fiber reinforced polymers have been widely used in engineering fields such as for civil, aeronautic, aerospace, automotive, civil engineering or naval industries thank to their high specific mechanical properties (high strength and high stiffness to weight ratio) and good fatigue resistance. The improvement and optimization of production technologies and processes permit also to reduce the assembly costs because polymer composites components are easy to make in a single sheet.

Nevertheless, in most of time, engineering structures are made of many components which have to be connected together. Two techniques are usually used to connect structural composite components: mechanical fastening using bolted or riveted joints and adhesive bonding. Especially in aircraft engineering, for security reasons and for improving fatigue properties, hybrid connections based on the combination of these two techniques are widely employed [1] [2] [3] [4].

This study being focused on polymer composite bolted joints, thus adhesive bonded joints and bolted/bonded joints are not studied and a particular attention is focused on metallic/composite bolted connections and hybrid joints.

The main disadvantage of bolted joints comes from the high stressed concentration zone near the fastener hole, which can reduce the stiffness and the ultimate strength due to damages in the composite material such as matrix cracking, fiber failure or plies delamination.

In literature, a lot of papers treat failure and damage prediction of the bolted joint. Experiments and numerical modelling of single-lap and double-lap, single and multi-bolted polymer composite joints have been investigated in numerous works [[5] [6] [7] [8] for instance]. Although, it is possible to reduce the stress level, avoid damage and increase the loads transfer by improving the local geo-

metry and the configuration of the bolted joint. This aspect is rarely treated in literature. Numerous parameters such as joint geometry, bolt diameter, washer diameter, clearance between the bolt and the composite plate, clamping force which induces a pre-stress in the bolt, and stacking sequence can have a great influence on the behavior, the stress state, the stiffness and the ultimate strength of the assembly.

The effect of washer size and tightening torque on a glass-epoxy bolted joint were studied in [9]. It was found that the strength increases with increasing washer size at a constant tightening torque. When the diameter of the washer decreases, lateral compressive stress in the composite material under the washer occurs and leads to micro-cracks around the hole. The stiffness of a glass-epoxy bolted joint increases with increasing tightening torque thanks to the increasing of contact pressure [9]. For single lap-shear glass-epoxy bolted joints, the failure load increases with the increasing of the clamping torque [10]. Fengrui *et al.* [11] studied a carbon-epoxy laminate single-lap bolted joint. The authors found that the bolt-hole clearance had a significant influence on the distribution of load while the bolt tightening torque had a negligible effect.

Muc *et al.* [12] studied a local reinforcement around the hole of a composite plate using curved fibres as the reinforced material, but the authors pointed out that this technique does not permit to recover the same strength of the composite material without hole, due to the great stress concentration factor in the vicinity of the hole. Yingdan *et al.* [13] proposed a variable angle tow placement technique to create local reinforcement on composites plates with holes. This technology consists in placing continuous fibers which follow the pre-calculated trajectories of eigenstresses.

However, these two technologies have not yet been applied to composite bolted joints.

A hybrid carbon-epoxy composite/titanium alloy assembled with a titanium bolt was studied in [14] [15] [16]. A local reinforcement around the hole was made with alternative carbon-epoxy and titanium alloy layers. It was found a significant increase of the strength of the bolted joint compared to this without metallic layers. A spacecraft payload adaptor was made with CFRP—titanium hybrid laminates and experimentally tested in [17]. The authors pointed out the advantages of this technology. They found a great increase of the load capability of bolted joints, the joint efficiency and the joint robustness. They also pointed out a high potential for steel reinforcement.

As describes above, most of time, the studied structure is composed of carbon-epoxy plates joined with a steel or titanium bolt. Glass-epoxy composites and hybrid metal/composite structures are less studied.

The association of glass-epoxy/stainless steel could replace with advantage stainless steel only components in industrial automotive applications such as transport of gas or liquid under pressure in order to reduce the weight of the vehicle and the cost of the transport. In this purpose, the aim of this paper is the

study of a single bolted joint under tension-compression made with two stainless steel sheets and a glass-epoxy material assembled with a pre-stress bolt.

The paper is organized as follows.

In the “Bolt joint” part, the general principle of the bolted joint studied, its geometry and the size of the sample used and materials chosen are described. Ten different configurations are proposed and defined. In the “Finite element modeling” part, calculi by finite elements method are performed to evaluate the stress state in the composite material. In the “stress analysis” part, in order to describe the increase of the tension-compression stress component in the most stressed zones of the composite material, the concept of stress concentration factor is exploited. All the ten configurations are analyzed and compared each other to select the best suited solution from a mechanical and technological point of view, taking into account the cost of machining of the bolted structure.

## 2. Bolt Joints

### 2.1. Materials and Specimen

The bolt joint of this study is based on the principle of the double lap bolted connection. It is designed as a multi-material assembly. In order to evaluate the stress concentration level in the bolted joint area, the model showed in **Figure 1** is used and subjected to tension-compression loads. All dimensions are specified in this figure.

The specimen is composed of (**Figure 2**):

- Two 316 L stainless steel external plates having a length of  $l_s = 150$  mm, a width of  $w_s = 50$  mm and a thickness of  $t_s = 5$  mm. A metallic bead is placed between the two plates (see **Figure 2**) in order to allow an efficient fixation of the specimen into the first grip of the testing machine in future experimental tests.

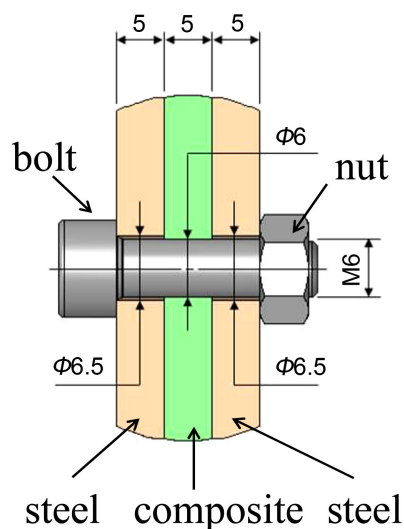


**Figure 1.** General definition of the bolted joint studied (size in mm). The washer between the nut and the metallic plate is non represented.

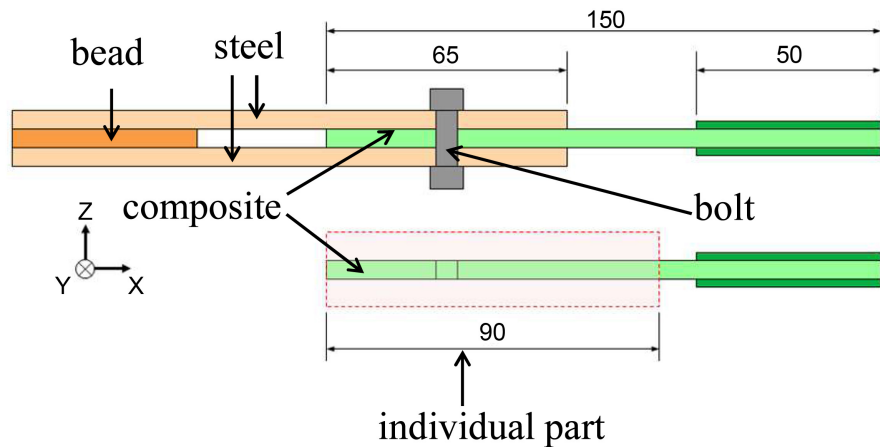


**Figure 2.** Design of the sample indicating all parts of the bolted joint.

- A 0/90 balanced woven glass-epoxy composite plate of the same size as the metallic plates, *i.e.* length  $l_c = 150$  mm, width  $w_c = 50$  mm and thickness  $t_c = 5$  mm. A symmetric stacking sequence with ten layers of same thickness ( $t_l = 0.5$  mm) is used to avoid undesired warping phenomenon during the tension or compression loading. Two beads are glued at the end of the composite plate in order to produce a balanced tension-compression loading by the second grip of the tensile machine.

The three plates of the bolt, *i.e.* two stainless steel sheets and the composite plate, are drilled and jointed together using a stainless steel M6 bolt of strength class A2-80. Its yield strength  $\sigma_{sb}$  is equal to 600 MPa and its ultimate strength  $\sigma_{mb}$  is equal to 800 MPa. The clearance between the composite material and the bolt is nil and this between the stainless steel plates and the bolt is equal to 0.5 mm. Since the fastener head and the nut washer are in contact with the steel sheets, there is no local crushing of the composite material which could damage it. The diameter of the washer has no influence on possible damage of composite since there is no contact between these two components.

The main function of the assembly described above is to transfer the load from the metallic part (stainless steel sheets) to the composite part (woven composite plate). For this reason, the analysis of the obtained results is mainly focused on the area around the bolt. Various designs of the bolted joint are studied and improvements are proposed leading to the lowest stress level in the composite material and taking into account technological aspects and cost.

Each specimen can be decomposed into a “standard part” which is the same for all configurations and an “individual part” which is specific to each configuration studied (**Figure 2**). The stress field is analyzed only in this “individual or central” part of the sample.

## 2.2. Configuration 1.1—Simple Bolted Joint

This technological solution showed in **Figure 1** is the simplest one and is treated later on as reference configuration.

### 2.3. Configurations 2.1 and 2.2—Bolted Joint with Aninsert

A metallic insert embedded in the composite material is introduced to improve the stress transfer through the bolted joint. Two configurations are studied.

A BigHead<sup>®</sup> insert is composed of a washer welded to a metallic element such as a threaded rod, a nail, a screw or a rod [18]. The BigHead<sup>®</sup> insert chosen for this study (Figure 3) is composed of a washer of diameter 23 mm welded to a M6 nut (configuration 2.1). It can be embedded into the composite material during the manufacturing process. Its role is to increase the binding between the different parts and to allow a better distribution of the load among the concerned plates. However, this kind of joint is non symmetric and applied load can lead to unwanted shear and bending stresses in the sample.

Configuration 2.2 is a bolted joint with a symmetric insert (Figure 4(a)) having a circular shape with a diameter of 30 mm and embedded into the woven 0/90 glass-epoxy composite. Each step of the insert is 0.5 mm high, the same as a ply of the composite, except for the central step whose height is equal to 1 mm (Figure 4(b)).

### 2.4. Configurations 3.1 and 3.2—“Waved” Bolted Joints

In order to increase the contact surface between the metallic and composite parts, the plates have here the same sinusoidal wave profiles. The load transfer should then be improved. The wave is defined by its half-period  $T/2 = 8$  mm and its amplitude. Two amplitudes  $h_1 = 2$  mm for configuration 3.1 and  $h_2 = 1$  mm for configuration 3.2 are studied (Figure 5).

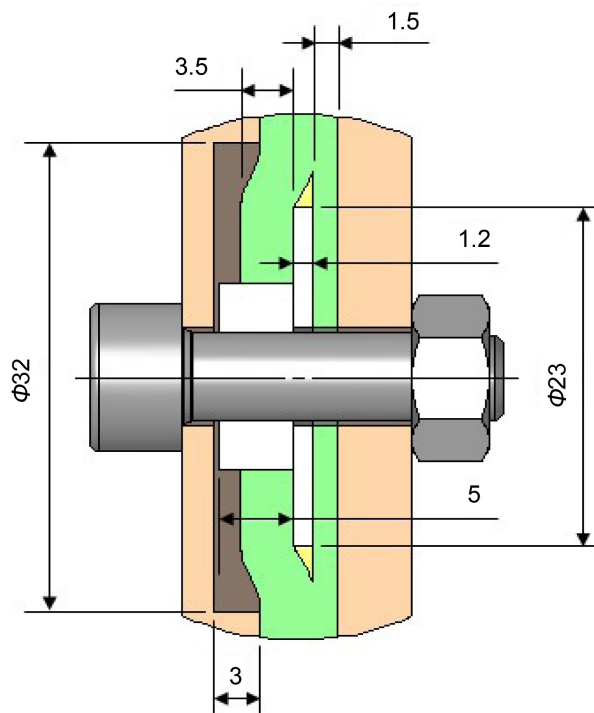
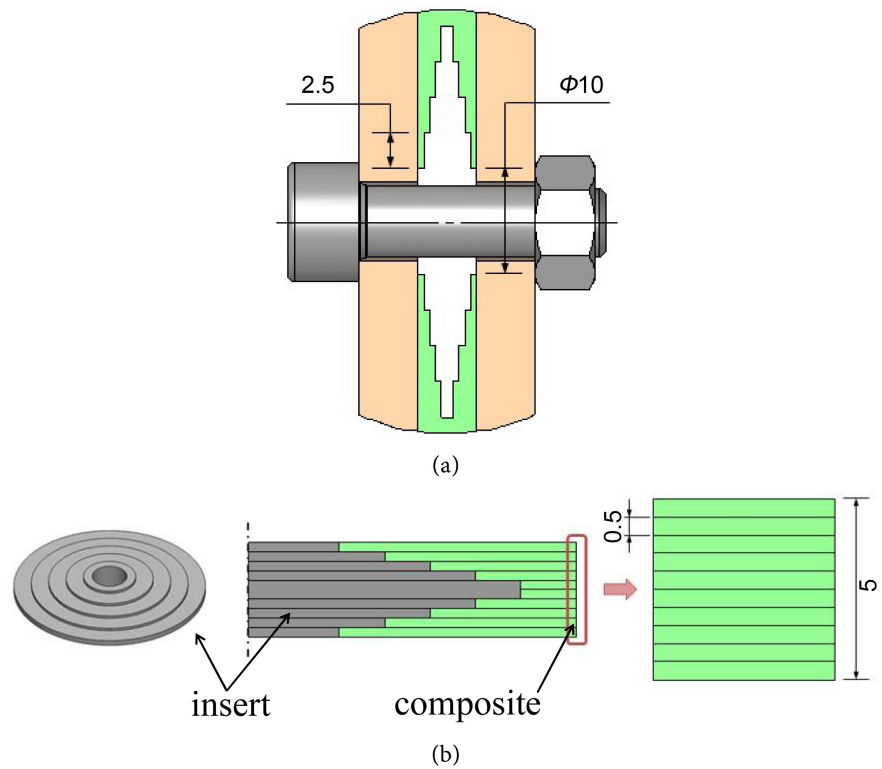
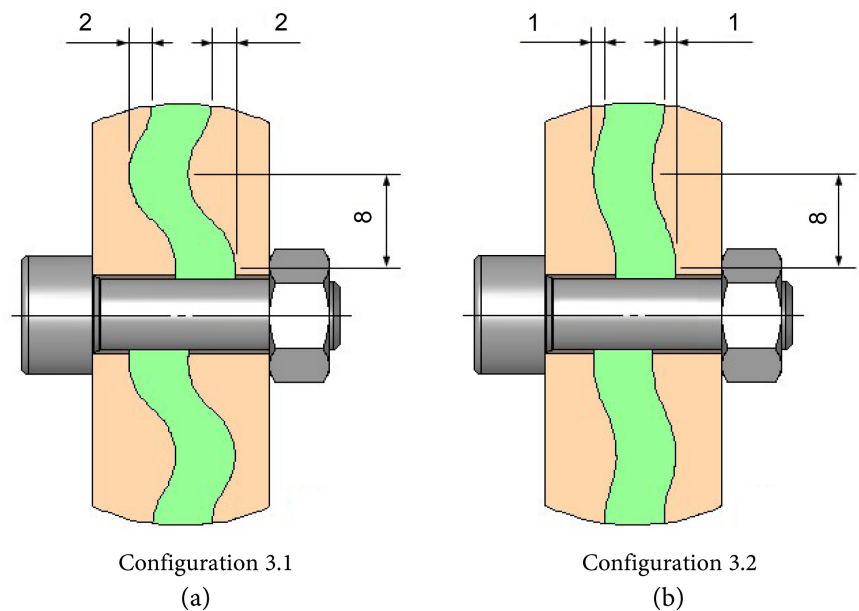


Figure 3. Configuration 2.1: BigHead<sup>®</sup> insert (all size in mm).



**Figure 4.** Configuration 2.2: bolted joint with a symmetric insert (all size in mm). (a) Configuration 2.2 with symmetric insert; (b) Configuration 2.2: dimensions of the layers.



**Figure 5.** Configurations 3.1 and 3.2: “Waved” bolted joints (all size in mm).

### 2.5. Configurations 4.1 to 4.3—Hybrid Composite Bolted Joints

In order to improve the mechanical characteristics of the bolted joint, a hybrid composite material defined by a succession of metallic and composites layers is studied. The stacking sequence is symmetric, composed of six 0/90 woven

glass-epoxy plies and four stainless steel layers. Each layer has the same thickness  $t_l = 0.5$  mm (Figure 6).

In order to avoid high stress concentration in the composite in the vicinity of the end of the metallic plate, a gradual transition of the length of the metallic layers is chosen. The metallic layers near the middle plane of the joint are 5 mm longer than the metallic plates (Figure 7).

Three hybrid composite bolted joints are studied (Figure 8):

- A simple hybrid composite bolted joint: Figure 8(a). (configuration 4.1)
- A hybrid composite bolted joint with a cylindrical sleeve of an external diameter  $d_{Is} = 10$  mm separating the bolt and the composite part (configuration 4.2). In this case, the metallic bolt remains in contact only with the metallic insert.

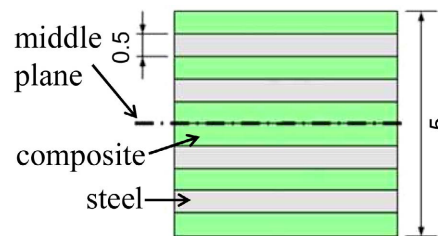


Figure 6. Stacking sequence of hybrid stainless steel/glass-epoxy composite material (all size in mm).

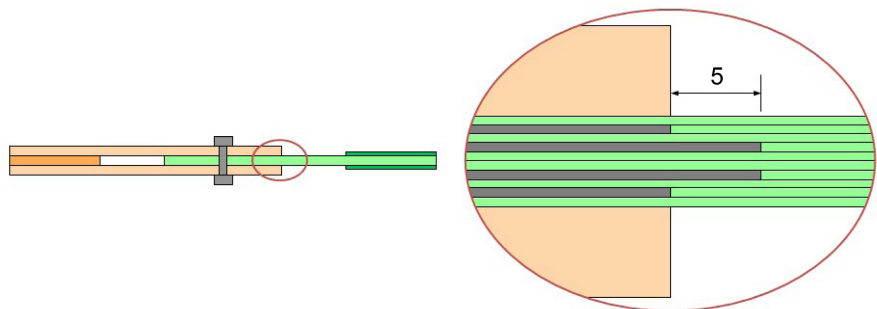


Figure 7. Metallic and composite layers at the end of metallic plates.

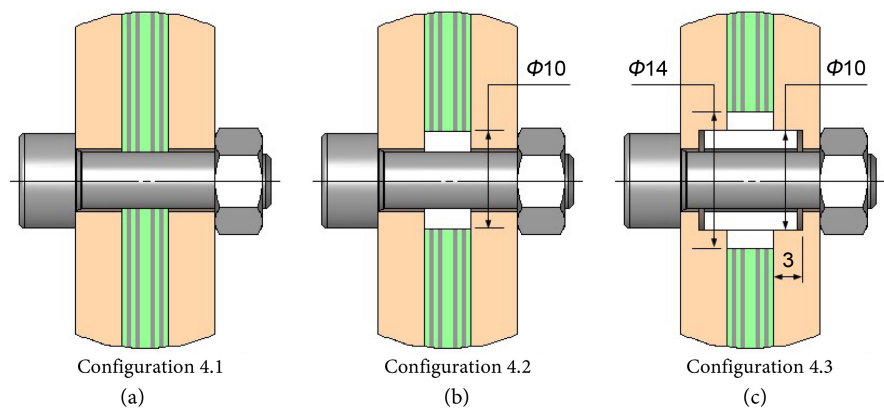


Figure 8. Hybrid composite bolted joints (all size in mm).



- A hybrid composite bolted joint with two sleeves and a shoulder (configuration 4.3). The first sleeve has the same external diameter as previously ( $d_{1s} = 10$  mm) and its thickness is greater than the thickness of the hybrid composite. The second sleeve has an external diameter  $d_{2s} = 14$  mm to avoid the contact between the hybrid composite and the metallic bolt (**Figure 8(c)**).

## 2.6. Configurations 5.1 to 5.2—Hybrid Composite Bolted Joints with a Stair-Insert

For this solution, the hybrid composite material is reinforced with a circular metallic stair-insert embedded in the composite in the vicinity of the bolt.

Two non-symmetric solutions are proposed:

- Hybrid composite bolted joint with a simple stair-insert (configurations 5.1) presented in **Figure 9(a)**. The insert has a circular shape and is embedded in the hybrid composite. This configuration is similar to 4.2 except that the insert has replaced the sleeve.
- Hybrid composite bolted joint with insert and sleeve (configurations 5.2) illustrated in **Figure 9(b)**. Configuration 5.2 is similar to 4.3 except that the insert has replaced the smallest sleeve.

## 3. Finite Element Modeling

Tension and compression tests are modelled using the finite element method. The software MSC Marc Mentat<sup>®</sup> is used. All the components of the bolted joints are modelled taken into account the particular constitutive behavior of the different materials, the non-linearity due to the contact (if existing) between the different sheets of the sample as well as the pre-stress in the bolt.

### 3.1. Meshing

A three dimensional model is built to simulate the bolt joint under tension or

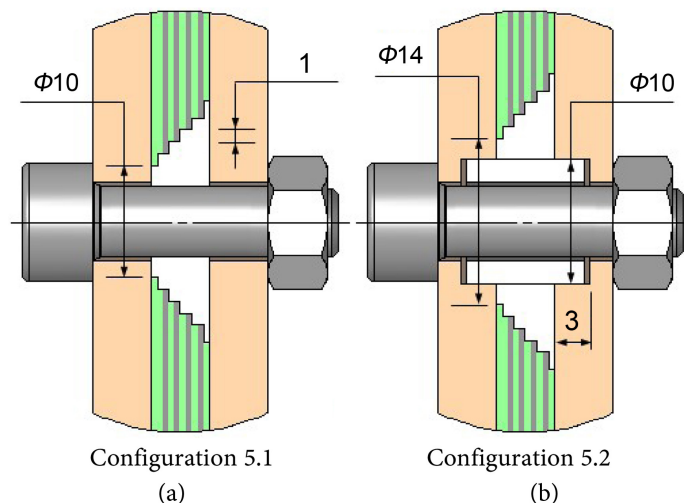


**Figure 9.** Hybrid composite bolted joint with a stair-insert (all size in mm).

compression. The specimens have been meshed with 8 nodes hexahedral elements using Hyper Mesh software.

The steel plates are modelled with 5 elements through the thickness, each element being 1 mm thick. Concerning the composite plate, the thickness of each element is chosen equal to those of each ply, *i.e.* 0.5 mm.

The mesh is sufficiently refined in the vicinity of the hole in the composite and steel plates in order to increase the accuracy in local area and predict the stress level correctly. For each configuration, ten tests are performed to ensure the convergence of the numerical solution.

**Figure 10** shows two typical examples of meshes of the “individual part” of the models (configurations 4.3 and 5.2).

### 3.2. Mechanical Constitutive Law of the Materials

The behavior of each material of the bolted joint is assumed to be homogeneous, elastic and linear.

The stainless steel is supposed isotropic with Young’s modulus  $E_{st} = 195,000$  MPa and Poisson’s ratio  $\nu_{st} = 0.3$ .

The balanced woven composite material is supposed orthotropic. Its characteristics are done in **Table 1** with respect to the coordinate system indicated in **Figure 2**.

### 3.3. Loading and Boundary Conditions

The tensile strength of the woven composite material is supposed to be equal to 500 MPa. The aim of this paper is to choose the most appropriate bolted joint.

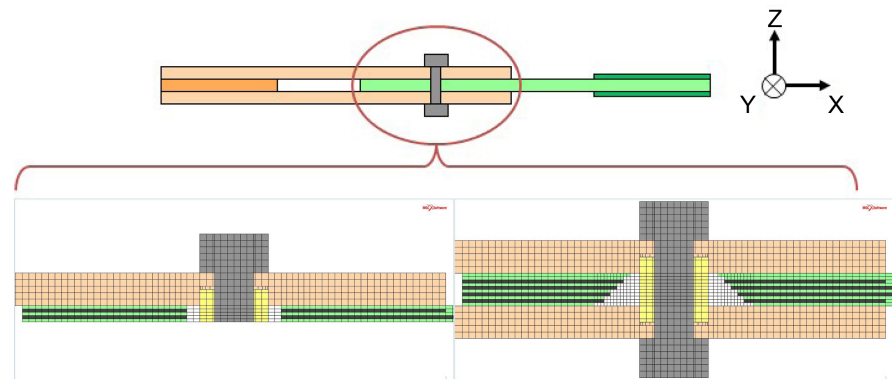


**Figure 10.** Example of meshes in the “individual part” of the sample. Case of two configurations 3.4 and 5.2.

**Table 1.** Mechanical properties of woven glass-epoxy composite material.

Young modulus (MPa)	Poisson ratio	Coulomb modulus (MPa)
$E_x$ : 26,000	$\nu_{xy}$ : 0.13	$G_{xy}$ : 5170
$E_y$ : 26,000	$\nu_{yz}$ : 0.34	$G_{yz}$ : 5050
$E_z$ : 10,750	$\nu_{zx}$ : 0.13	$G_{xz}$ : 5050

The damage and fracture are not considered during the analysis of obtained results. Consequently, the applied nominal tensile or compressive stress is limited to 70% of the material strength, *i.e.* is supposed to be  $\sigma_{xx}^{nom} = \pm 350$  MPa.

In order to reduce the computation time, only a quarter or a half of the sample is modeled depending on the symmetries of the configuration studied, namely:

- A quarter of the sample is modeled for configurations 1.1, 4.1 to 4.3 and 5.1.
- A half of the sample is modeled for configurations 2.1, 3.1 and 3.2, 5.2 and 5.3.

### 3.4. Clamping Force

Every bolted joint, which has to transmit forces between components, can only work with a reliable and sufficient preload or clamping force. Several studies showed that clamping force can affect failure mode and ultimate strength of a bolt joint [[19] [20] for instance]

For this reason, a clamping force is taken into account in this research in order to evaluate the stress level in the composite material of the bolted joint. It is generated by a pre-stress in the bolt.

The pre-stress is usually taken equal to 90 percent of the yield stress of the bolt material. In the current study, the bolt class A2-80 was considered with a yield stress equal to 600 MPa and an ultimate stress equal to 800 MPa. Accordingly, the maximal pre-stress in the bolt is then 540 MPa.

In order to generate the pre-stress, a thermal loading step is used. To simulate tightening stress on the bolted joint, a negative uniaxial thermal strain is engendered in bolt using the linear thermal expansion of the material:

$$\bar{\varepsilon}^{th} = \bar{\alpha} \Delta T \quad (1)$$

where  $\Delta T$  is the negative increment of temperature and

$\bar{\alpha}$  is a tensor of expansion coefficients such that only the component  $\alpha_{33}$  is non nil:

$$\bar{\alpha} = \begin{pmatrix} 0 & 0 & 0 \\ 0 & 0 & 0 \\ 0 & 0 & \alpha_{33} \end{pmatrix} \quad (2)$$

Such a tensor enables avoiding undesired thermal expansion in transverse directions of the bolt studied.

The value of  $\Delta T$  is chosen to obtain the desired pre-stress in the bolt.  $\Delta T = -277$  K was necessary to obtain a pre-stress equal to 540 MPa using:

$$\alpha_{33} = 10^{-5} / \text{K}.$$

### 3.5. Contacts

The bolted joint is constituted of two types of materials, metallic and composite. Some contacts are managed between the different parts and the materials.

For a steel/steel contact, a friction coefficient equal to 0.1 has been used. For a

steel/glass-epoxy composite, a friction coefficient equal to 0.6 has been applied [21].

## 4. Stress Analysis

### 4.1. Stress Discontinuities in the Components of the Bolted Joint

The stresses are analyzed in the “individual” parts of the bolted joints. The woven compositematerial of the bolted joint described in sub-sections 2.1 to 2.4 is composed of ten plies of same thickness that are supposed to be perfectly bonded one to each other. In the case of a hybrid bolted joint described in sub-sections 2.5 and 2.6, the adjacent layers of stainless steel plies and composite plies are also supposed to be perfectly bonded. Due to the misorientation of the plies constituting the woven glass-epoxy composite material or the difference of elastic properties of the glass-epoxy composite and the stainless steel, some stress tensor components are not necessarily continuous through the interface between two consecutive layers.

In fact, from a mechanical point of view, the stress vector  $\vec{T}$  should be continuous through each interface:

$$\vec{T} = \bar{\bar{\sigma}} \vec{n} \quad (3)$$

where  $\bar{\bar{\sigma}}$  is the stress tensor and  $\vec{n}$  the unit vector normal to the interface.

Let's consider two adjacent layers denoted (1) and (2) respectively, composed of two different materials, the  $z$  direction being perpendicular to the interface separating both layers.

Since  $\vec{T}^{(1)} = \vec{T}^{(2)}$ , one obtains:

$$\Rightarrow \bar{\bar{\sigma}}^{(1)} \vec{n} = \bar{\bar{\sigma}}^{(2)} \vec{n} \quad (4)$$

where  $\bar{\bar{\sigma}}^{(1)}$  and  $\bar{\bar{\sigma}}^{(2)}$  are the stress tensors in materials (1) and (2) respectively and

$$\vec{n} = \begin{Bmatrix} 0 \\ 0 \\ 1 \end{Bmatrix} \quad (5)$$

Consequently, it comes that:

$$\sigma_{xz}^{(1)} = \sigma_{xz}^{(2)}, \quad \sigma_{yz}^{(1)} = \sigma_{yz}^{(2)} \quad \text{and} \quad \sigma_{zz}^{(1)} = \sigma_{zz}^{(2)} \quad (6)$$

It appears that the three components calculated above are continuous while the components  $\sigma_{xx}$ ,  $\sigma_{yy}$ , and  $\sigma_{xy}$  can be discontinuous.

In finite element method, stress components are calculated at the Gauss' points of each element. The number and location of these points depend on the element type used. For hexahedral 8 node-elements, in the case of full integration technology, the stress and strain tensors are evaluated in 8 Gauss' points. In order to correctly evaluate the stress state in each layer, taking into account the possible discontinuities, the stress state of the given integration point is translated to the nearest node of each element.

## 4.2. Stress Concentration Factors

The analysis is focused on stress state in the composite part of the bolted joint.

It is obvious that stresses are increased in the vicinity of the hole when the bolted joint is loaded under tension or compression [22]. Stresses can also be increased in the area of the interface of the composite material and the stainless steel due to the change of material stiffness (see sub-section 4.1).

The simplest way to evaluate the local stress increase, and to compare the behavior of the different bolted joints described in section 2, is the use of stress concentration factor concept.

For a monotonic loading, two different stress concentration factors that describe increase of  $\sigma_{xx}$  stress component in the composite material are defined:

The stress concentration factors for a tension loading denoted  $K_t$  is defined as follows:

$$K_t = \frac{\sigma_{xx}^{max}}{\sigma_{xx}^{nom}} \quad \text{where } \sigma_{xx}^{nom} \text{ is equal to 350 MPa} \quad (7)$$

the stress concentration factors for a compression loading denoted  $K'_t$  is defined as follows:

$$K'_t = \frac{\sigma_{xx}^{min}}{\sigma_{xx}^{nom}} \quad \text{where } \sigma_{xx}^{nom} \text{ is equal to } -350 \text{ MPa} \quad (8)$$

As composite materials can be sensitive to fatigue, the stress concentration factor for a cyclic loading with a ratio  $R = -1$ , denoted  $K_{\Delta\sigma}$  is defined as follows:

$$K_{\Delta\sigma} = \frac{\sigma_{xx}^{max} - \sigma_{xx}^{min}}{2\sigma_{xx}^{nom}} \quad \text{where } 2\sigma_{xx}^{nom} \text{ is equal to 700 MPa} \quad (9)$$

## 5. Results and Discussion

Stress concentration factors  $K_t$ ,  $K'_t$  and  $K_{\Delta\sigma}$  in the composite part are calculated using finite element method for each configuration described at section 2. Analyzes take into account the location of maximal stresses which can be the vicinity of the hole in the composite, the vicinity of the circumference of the metallic insert or the vicinity of the end of the biggest metallic ply.

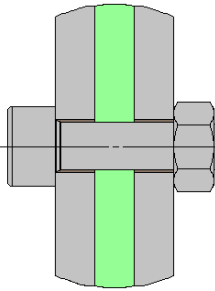
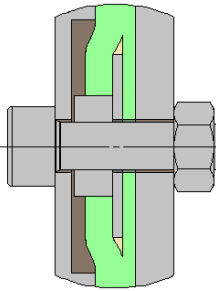
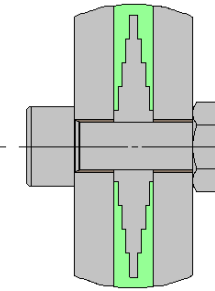
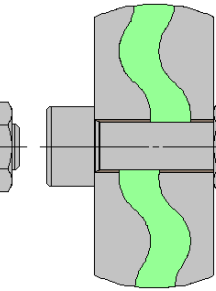
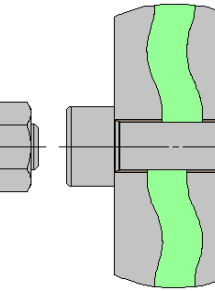
**Figures 12-16** give for each configuration the color maps of  $\sigma_{xx}$  stress component and the values of stress concentration factors  $K_t$  and  $K'_t$ . The location of the most stressed point is also identified in these figures. **Table 2** and **Table 3** compare the values of stress concentration factors for all configurations.

**Figure 11** shows an example of color map and the zones denoted (a) et (b) which can be the most stressed ones depending on the configuration studied.

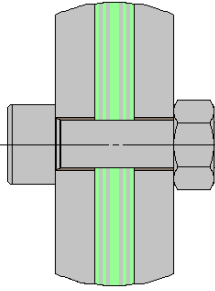
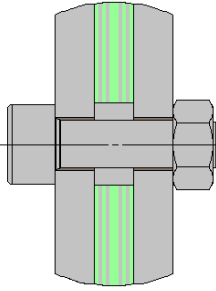
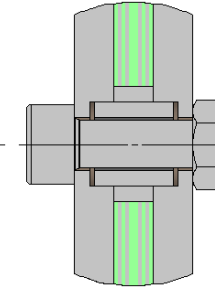
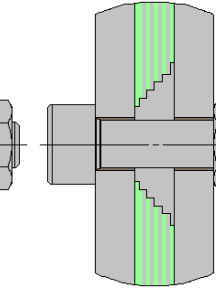
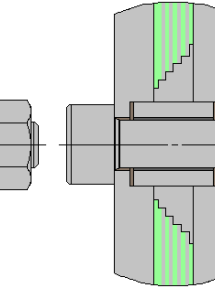
### 5.1. Simple Bolted Joint

Obvious results are obtained for the simple bolted joint (configuration 1.1). High concentration factors are identified which are located at the circumference of the hole, in the  $(x, z)$  symmetry plane.

**Table 2.** Concentration factors for configurations 1.1 to 3.2.

configuration					
	1.1	2.1	2.2	3.1	3.2
$K_t$	12.6	3.7	2	5.7	5.8
$K_r$	9.7	3.6	2	2.7	4.1
$K_{\Delta\sigma}$	8.9	3.6	2	3.1	3.1

**Table 3.** Concentration factors for configurations 4.1 to 5.2.

configuration					
	4.1	4.2	4.3	5.1	5.2
$K_t$	3.6	1.3	1.3	1.3	1.3
$K_r$	5	1.4	1.4	1.3	1.3
$K_{\Delta\sigma}$	2.5	1.3	1.3	1.3	1.3

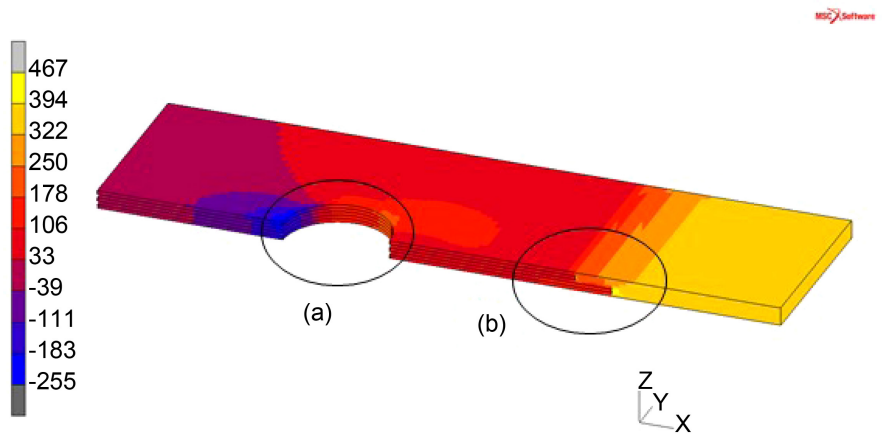


**Figure 11.** Example of color map of  $\sigma_{xx}$  stress component (MPa).

Very large values of  $K_t$  equal to 12.6 and  $K'_t$  equal to 17.8 have been obtained, see **Figure 12**. The cyclic concentration factor is close to 9. They are due to the localized transfer of load from the bolt to the composite material. Since there is no clearance between the bolt and the composite plate, the stress concentration factor in compression  $K'_t$  is higher than  $K_t$ . Such a technological solution is not adapted for the highly loaded joints.

### 5.2. Bolted Joint with an Insert

Configurations 2.1: The maximal and minimal stresses are located at the circumference of the insert washer. The BigHead<sup>®</sup> insert improves the load transfer. Indeed, the stress concentration factors are significantly smaller than those of simple bolted joint.  $K_t$  and  $K'_t$  equals 3.7 and 3.6 respectively (**Figure 13**). The cyclic concentration factor  $K_{\Delta\sigma}$  is also equal to 3.6. The use of BigHead<sup>®</sup> insert decreases all the concentration factors by nearly three compared to the previous solution. However, the discontinuous variation of the stiffness between the insert and the composite plate still generates the local stress concentration well distinguishable in **Figure 13**.

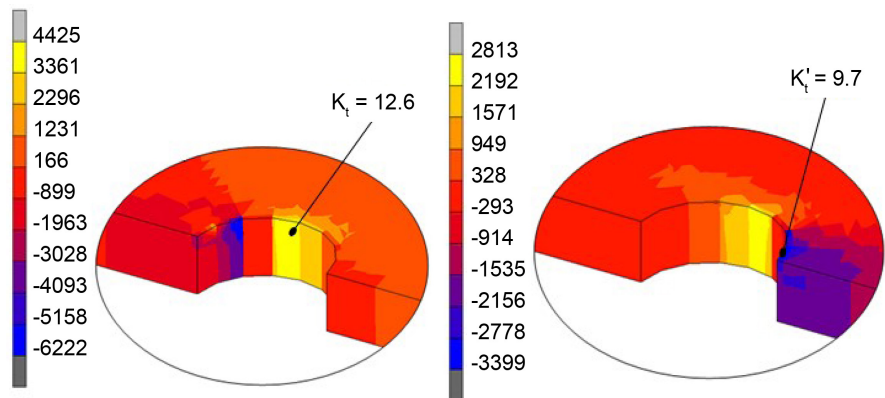


**Figure 12.** Color map of  $\sigma_{xx}$  stress component (MPa) and stress concentration factors for configuration 1.1 (simple bolted joint).

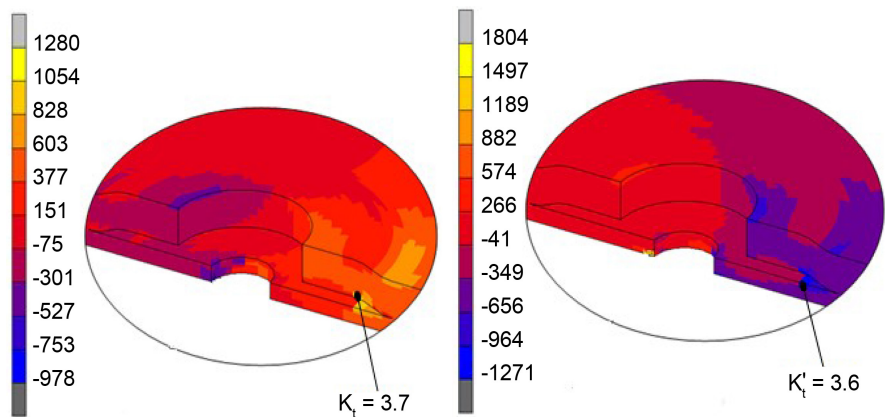


**Figure 13.** Color map of  $\sigma_{xx}$  stress component (MPa) and stress concentration factors for configuration 2.1 (BigHead<sup>®</sup> insert).

Configurations 2.2: In order to obtain a gradual transition between the different parts of the bolted joint, an insert with steps is used around the bolt (**Figure 14**). As in the case of BigHead<sup>R</sup> insert, maximal and minimal stresses are located at the circumference of the insert, in the vicinity of its greatest radius. Stress concentration factors are not so high as for BigHead<sup>R</sup> Insert.  $K_t$ ,  $K'_t$  and  $K_{\Delta\sigma}$  are equal to 2 (instead 3.7 and 3.6, see last paragraph).

### 5.3. Waved Bolted Joint

Configuration 3.1: The amplitude of the wave is 1 mm and the maximal stress occurs at the vicinity of the hole, in the same way as in the simple bolted joint. This configuration is an improvement of configuration 1.1, but the stress concentration factors are relative high:  $K_t$  is equal to 5 for a tension loading and the value of  $K_{\Delta\sigma}$  is close to 3 (**Figure 15(a)**). In fact, the wave effect is here not sufficient to reduce significantly the stress level in the composite.

Configuration 3.2: The amplitude of the wave is 2 mm and the stress concentration factors are quite similar to those of configuration 3.1. Nevertheless, the maximal stress is not located at the vicinity of the hole but at the top of the first half-period of the wave (**Figure 15(b)**). This phenomenon is due to the too small radius of the wave.

Configurations 3.1 and 3.2 have stress concentration factors smaller than those of configuration 1.1 thanks to the waves but seem however to be not satisfactory.

### 5.4. Hybrid Composite Bolted Joint

Configuration 4.1: A way to reduce the stress level and the stress concentration factor in the vicinity of the hole can be found by adding metallic plies in the composite material [14] [15] [16] [17]. The highest  $\sigma_{xx}$  stress is again located at the vicinity of the hole, here in the first composite ply (**Figure 16(a)**). In fact, from a geometrical point of view, configurations 1.1 and 4.1 are quite similar. Stress concentration factors are not so high for configuration 4.1 thanks to metallic plies that reinforce the composite.  $K_t$  equals 3.6 and  $K_{\Delta\sigma}$  is equal to 2.5.

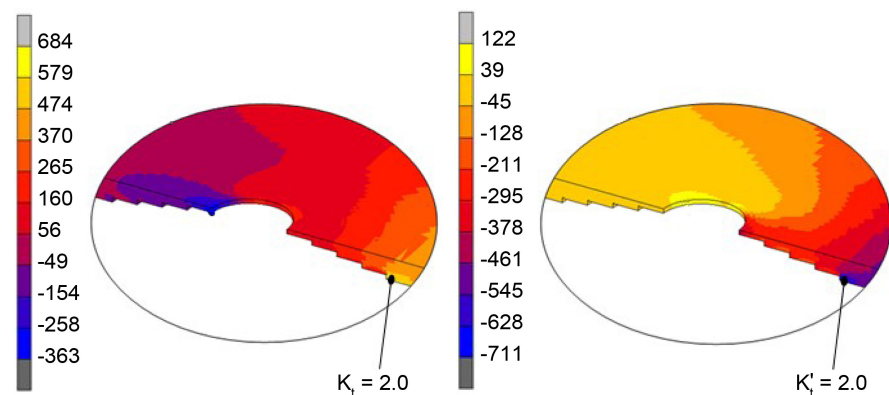


**Figure 14.** Color map of  $\sigma_{xx}$  stress component (MPa) and stress concentration factors for configuration 2.2 (bolted joint with an insert).



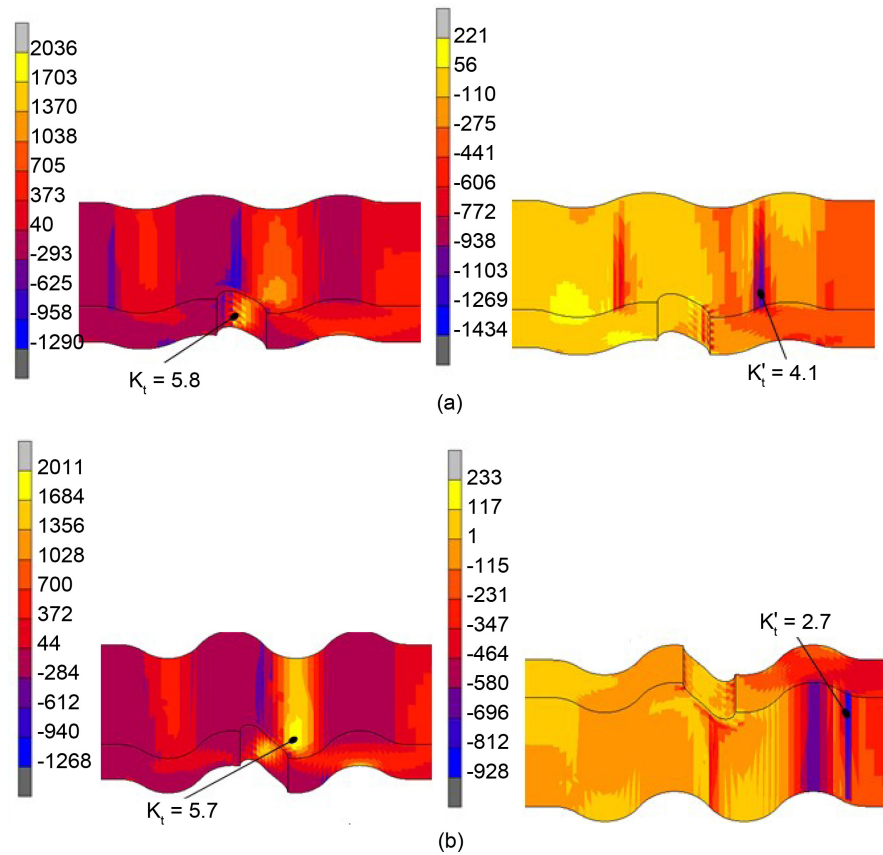


**Figure 15.** (a): Color map of  $\sigma_{xx}$  stress component (MPa) and stress concentration factors for configuration 3.1 (waved bolted joint). (b): Color map of  $\sigma_{xx}$  stress component (MPa) and stress concentration factors for configuration 3.2 (waved bolted joint).

In the same way as for configuration 1.1, the absence of clearance between the bolt and the composite material induces  $K'_t$  higher than  $K_t$ . Configuration 4.1 is better compared to configuration 1.1, but still remains not satisfactory.

Configuration 4.2: Another way to reduce the stress level in the composite part is obtained by using a sleeve around the bolt. In this case, the stress concentration factors are small, the values obtained for  $K_t$  and  $K_{\Delta\sigma}$  are equal to 1.4, which is an acceptable level (**Figure 16(b)**). It should be noted that thanks to the presence of the sleeve, maximal stress in tension and minimal stress in compression don't occur at the vicinity of the hole because there isn't any contact between the composite part and the bolt. They are both localized at the end of the longest metallic ply.

Configuration 4.3: Configuration 4.2 can be modified by adding a second sleeve around the bolt. This corresponds to configuration 4.3. The stress state in the composite part is quite similar to those for configuration 4.2 and the stress concentration factors  $K_t$ ,  $K'_t$  and  $K_{\Delta\sigma}$  have approximately the same values.

They are at most equal to 1.4 for both configurations 4.2 and 4.3 which is an acceptable value. One can say that these two configurations are satisfactory.

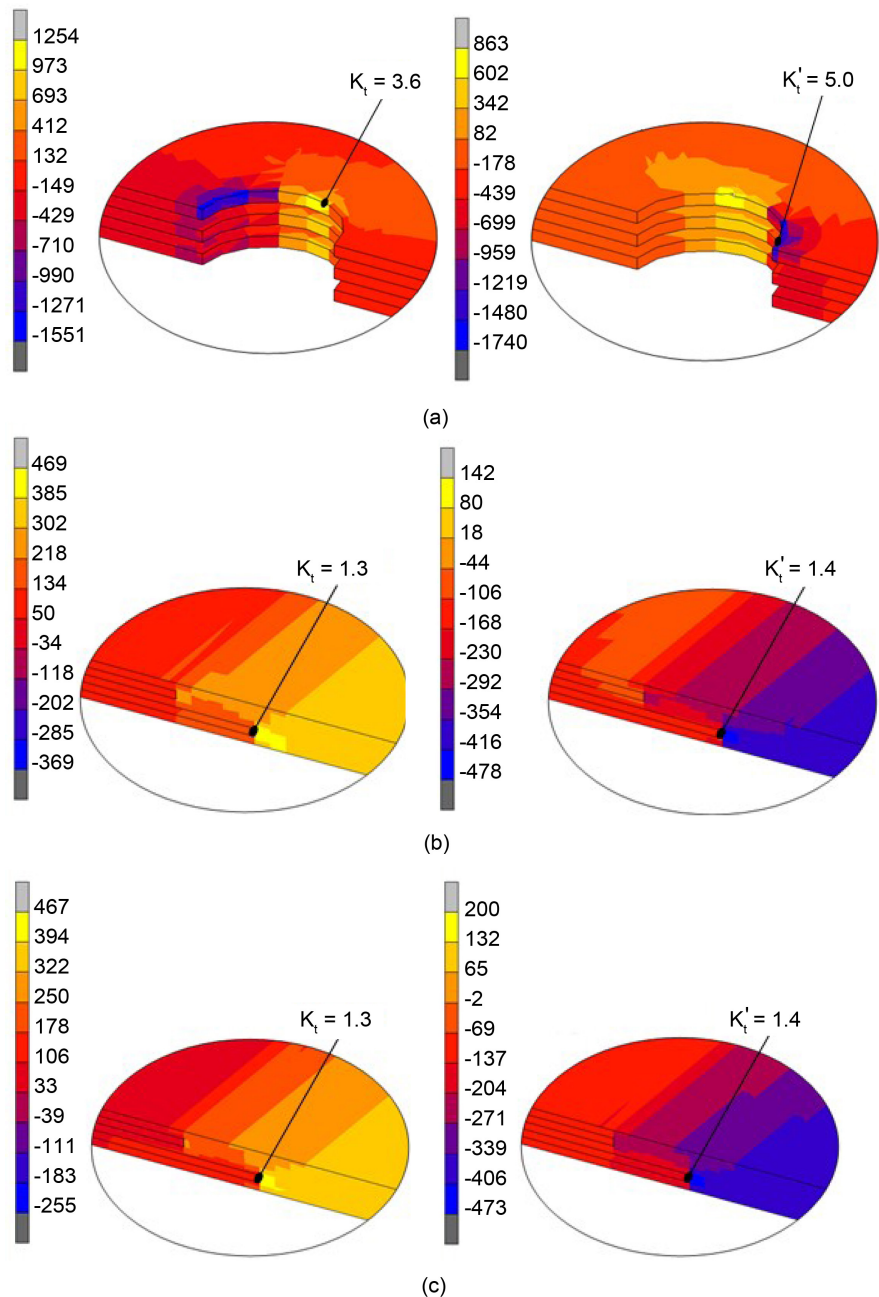


**Figure 16.** (a): Color map of  $\sigma_{xx}$  stress component (MPa) and stress concentration factors for configuration 4.1. (b): Color map of  $\sigma_{xx}$  stress component (MPa) and stress concentration factors for configuration 4.2. (c) Color map of  $\sigma_{xx}$  stress component (MPa) and stress concentration factors for configuration 4.3.

### 5.5. Hybrid Composite Bolted Joint with an Insert

Configurations 2.1 and 2.2 showed that an insert could improve a simple bolted joint by reducing stress concentration factors. Configuration 4.2 and 4.3 showed that the use of one or two sleeves improves the behavior of a simple hybrid bolted joint (configuration 4.1).

The idea is here to combine and to take advantage of these two solutions, in-

sert and hybrid composite material, to improve the bolted joint.

For both configurations 5.1 and 5.2, stress in tension and stress in compression are maximal and minimal at the end of the longest composite ply. The stress concentration factors have the same values as those obtained for configurations 4.2 and 4.3. In fact, for these four configurations, the direct contact between the hybrid composite material and the bolt was avoided. The use of sleeves or stepped inserts does not change the stress state in the composite part: the values of stress concentration factors and the location of maximal stresses remained the same. In the same way as for configurations 4.2 and 4.3, configurations 5.1 and 5.2 are satisfactory.

## 6. Conclusions

Among the ten tested configurations, the 4.2, 4.3, 5.1 and 5.2 ones are acceptable with respect to the conventional values of stress concentration factors of less than 2. These configurations are made with hybrid composite bolted joints and sleeve or insert. In fact, thanks to these parts, there is no direct contact between composite material and metallic bolt. The maximal stresses don't occur in the vicinity of the hole, but at the end of the longest metallic ply. As consequence, the stress concentration factors  $K_t$ ,  $K'_t$  and  $K_{\Delta\sigma}$  are at most equal to 1.4. It should be noted that a low stress concentration factor in fatigue  $K_{\Delta\sigma}$  should be required for most applications such as aeronautic and automotive ones, because these structures are most of time submitted to cyclic loadings.

Overall, a bolted joint is intended to be easy and inexpensive to produce. The shape of insert of configurations 5.1 and 5.2 make them expensive to machine. For this reason, the solutions 5.1 and 5.2 are less interesting than the configurations 4.2 and 4.3.

The stress concentration factors for these two cases have about the same values, however the configuration 4.3 should be preferred since it is less loaded thanks to the shoulder.

In a next work, the configuration 4.3 will be experimentally tested at room, but also at cryogenic temperatures.

Indeed, stainless steel/glass-epoxy bolted joints such that of this study can be used as components of cryogenic devices such as fastener of liquefied gas tank or in the design of semi-trailers for transport of liquefied gas [23].

## Conflicts of Interest

The authors declare no conflicts of interest regarding the publication of this paper.

## References

- [1] Lim, G.-H., Bodjona, K., Raju, K.P., *et al.* (2018) Evolution of Mechanical Properties of Flexible Epoxy Adhesives under Cyclic Loading and Its Effects on Composite Hybrid Bolted/Bonded Joint Design. *Composite Structures*, **189**, 54-60. <https://doi.org/10.1016/j.compstruct.2018.01.049>

- [2] Lopez-Cruz, P., Laliberté, J. and Lessard, L. (2017) Investigation of Bolted/Bonded Composite Joint Behaviour Using Design of Experiments. *Composite Structures*, **170**, 192-201. <https://doi.org/10.1016/j.compstruct.2017.02.084>
- [3] Khashaba, U.A. (2018) Static and Fatigue Analysis of Bolted/Bonded Joints Modified with CNTs in CFRP Composites under Hot, Cold and Room Temperatures. *Composite Structures*, **194**, 279-291. <https://doi.org/10.1016/j.compstruct.2018.04.008>
- [4] Marannano, G. and Zuccarello, B. (2015) Numerical Experimental Analysis of Hybrid Double Lap Aluminum-CFRP Joints. *Composites Part B: Engineering*, **71**, 28-39. <https://doi.org/10.1016/j.compositesb.2014.11.025>
- [5] Liu, F.R., Lu, X.H., Zhao, L.B., Zhang, J.Y., Xu, J.F. and Hu, N. (2018) Investigation of Bolt Load Redistribution and Its Effect on Failure Prediction in Double-Lap, Multi-Bolt Composite Joints. *Composite Structures*, **202**, 397-405. <https://doi.org/10.1016/j.compstruct.2018.02.043>
- [6] Mandal, B. and Chakrabarti, A. (2018) Numerical Failure Assessment of Multi-Bolt FRP Composite Joints with Varying Sizes and Preloads of Bolts. *Composite Structures*, **187**, 169-178. <https://doi.org/10.1016/j.compstruct.2017.12.048>
- [7] Nerilli, F. and Vairo, G. (2017) Progressive Damage in Composite Bolted Joints via a Computational Micromechanical Approach. *Composites Part B: Engineering*, **111**, 357-371. <https://doi.org/10.1016/j.compositesb.2016.11.056>
- [8] Hua, X.F., Haris, A., Ridha, M., Tan, V.B.C. and Tay, T.E. (2018) Progressive Failure of Bolted Single-Lap Joints of Woven Fiber-Reinforced Composites. *Composite Structures*, **189**, 443-454. <https://doi.org/10.1016/j.compstruct.2018.01.104>
- [9] Khashaba, U.A., Sallam, H.E.M., Al-Shorbagy, A.E. and Seif, M.A. (2006) Effect of Washer Size and Tightening Torque on the Performance of Bolted Joints in Composite Structures. *Composite Structures*, **73**, 310-317. <https://doi.org/10.1016/j.compstruct.2005.02.004>
- [10] Choia, J., Hashemini, S.M., Chun, H.-J., Park, J.-C. and Chang, H.S. (2018) Failure Load Prediction of Composite Bolted Joint with Clamping Force. *Composite Structures*, **189**, 247-255. <https://doi.org/10.1016/j.compstruct.2018.01.037>
- [11] Liu, F.R., Lu, X.H., Zhao, L.B., Zhang, J.Y., et al. (2018) An Interpretation of the Load Distributions in Highly Torqued Single-Lap Composite Bolted Joints with Bolt-Hole Clearances. *Composites Part B: Engineering*, **138**, 194-205. <https://doi.org/10.1016/j.compositesb.2017.11.027>
- [12] Muc, A. and Ulatowska, A. (2012) Local Fibre Reinforcement of Holes in Composite Multilayered Plates. *Composite Structures*, **94**, 1413-1419. <https://doi.org/10.1016/j.compstruct.2011.11.017>
- [13] Zhu, Y.D., Qin, Y.L., Qi, S.J., Xu, H.B., Liu, D. and Yan, C. (2018) Variable Angle Tow Reinforcement Design for Locally Reinforcing an Openhole Composite Plate. *Composite Structures*, **202**, 162-169. <https://doi.org/10.1016/j.compstruct.2018.01.021>
- [14] Kolesnikov, B., Herbeck, L. and Fink, A. (2008) CFRP/Titanium Hybrid Material for Improving Composite Bolted Joints. *Composite Structures*, **83**, 368-380. <https://doi.org/10.1016/j.compstruct.2007.05.010>
- [15] Camanho, P.P., Fink, A., Obst, A. and Pimenta, S. (2009) Hybrid Titanium-CFRP Laminates for High-Performance Bolted Joints. *Composites Part A: Applied Science and Manufacturing*, **40**, 1826-1837. <https://doi.org/10.1016/j.compositesa.2009.02.010>

- [16] Kolks, G. and Tserpes, K.I. (2014) Efficient Progressive Damage Modeling of Hybrid Composite/Titanium Bolted Joints. *Composites Part A: Applied Science and Manufacturing*, **56**, 51-63. <https://doi.org/10.1016/j.compositesa.2013.09.011>
- [17] Fink, A., Camanho, P.P., Andrés, J.M., Pfeiffer, E. and Obst, A. (2010) Hybrid CFRP/Titanium Bolted Joints: Performance Assessment and Application to a Spacecraft Payload Adaptor. *Composites Science and Technology*, **70**, 305-317. <https://doi.org/10.1016/j.compscitech.2009.11.002>
- [18] BigHead®. <https://www.bighead.co.uk>
- [19] Sasikumar, A., Guerrero, J.M., Quintanas-Corominas, A. and Costa, J. (2021) Numerical Study to Understand Thermo-Mechanical Effects on a Composite Aluminium Hybrid Bolted Joint. *Composite Structures*, **275**, Article ID: 114396. <https://doi.org/10.1016/j.compstruct.2021.114396>
- [20] Choi, J., Hasheminia, S.M., Chun, H.-J., Park, J.-C. and Chang, H.S. (2018) Failure Load Prediction of Composite Bolted Joint with Clamping Force. *Composite Structures*, **189**, 247-255. <https://doi.org/10.1016/j.compstruct.2018.01.037>
- [21] Larsen, T., *et al.* (2007) Comparison of Friction and Wear for an Epoxy Resin Reinforced by a Glass or a Carbon/Aramid Hybrid Weave. *Wear*, **262**, 1013-1020. <https://doi.org/10.1016/j.wear.2006.10.004>
- [22] Cabrera-González, J.A., Vargas-Silva, G. and Barroso, A. (2021) Riveted Joints in Composites, a Practical Tool to Estimate Stresses around the Rivet Hole. *Composite Structures*, **263**, Article ID: 113735. <https://doi.org/10.1016/j.compstruct.2021.113735>
- [23] Lee, K.H. and Lee, D.G. (2010) Design of a Hybrid Glass Composite Anchor for LNG Cargo Containment Systems. *Composite Structures*, **92**, 469-479. <https://doi.org/10.1016/j.compstruct.2009.08.031>